

NATIONAL ADVISORY COMMITTEE FOR AERONAUTICS

TECHNICAL NOTE 3703

THE FLOW PAST AN UNSWEPT- AND A SWEPT-WING—BODY
COMBINATION AND THEIR EQUIVALENT BODIES OF
REVOLUTION AT MACH NUMBERS NEAR 1.0

By Walter F. Lindsey

Langley Aeronautical Laboratory
Langley Field, Va.



Washington

June 1956

NATIONAL ADVISORY COMMITTEE FOR AERONAUTICS

TECHNICAL NOTE 3703

THE FLOW PAST AN UNSWEPT- AND A SWEPT-WING-BODY
COMBINATION AND THEIR EQUIVALENT BODIES OF
REVOLUTION AT MACH NUMBERS NEAR 1.0¹

By Walter F. Lindsey

SUMMARY

Tests utilizing the schlieren method of flow photography have been conducted to provide a comparison of the complete flow fields past an unswept- and a swept-wing-body combination and the flow fields past their equivalent bodies of revolution at Mach numbers around 1.0. The results indicated that the shock growth and positions on the wing-body combinations were closely reproduced in the flow past the equivalent body.

INTRODUCTION

The correspondence of drag between a wing-body combination and its equivalent body of revolution as determined by the transonic "area rule" was stated in reference 1 to require a correspondence of the flow fields and shock formation about the two bodies. Some limited information on the flow fields in reference 1 indicated that such a condition existed. In the absence of information whereby a comparison of the complete flow fields past a wing-body combination and its equivalent body could be made, tests utilizing the schlieren method of flow photography have been conducted to provide this information by examining the complete flow fields and the shock formations existing on two wing-body combinations and their equivalent bodies.

APPARATUS AND TESTS

The tests were conducted in the Langley 4- by 19-inch semiopen tunnel (ref. 2), which had been modified to operate on a direct-blowdown

¹Supersedes recently declassified NACA Research Memorandum L54A28a by Walter F. Lindsey, 1954.

principle. A support sting whose diameter was equal to the body diameter at the body-sting juncture and increased downstream (fig. 1) was installed in the tunnel. All models involved in this investigation were supported at an angle of attack of 0° on the sting.

The models consisted of body alone, two wing-body combinations, and their equivalent bodies. The basic body used in all combinations had a fineness ratio of 12 and a profile as shown in figure 1(a). The wing of one combination was a 45° sweptback wing having a taper ratio of 1 and an aspect ratio of 3.9. The wing had an NACA 66-006 airfoil section in a streamwise direction. The equivalent body had the same longitudinal area distribution and is shown in figure 1. The wing of the second wing-body combination was an unswept wing having a taper ratio of 1 and an aspect ratio of 1.5. The wing had a 6-percent-thick symmetrical circular-arc profile with maximum thickness at 50 percent chord. The profile and area distribution of the equivalent body for this combination are also shown in figure 1. The profiles of the equivalent bodies for both wing-body combinations can be compared in figure 1(a). The bump on the basic body formed by the addition of the cross-sectional area of the swept wing, in accordance with the transonic area rule (ref. 1), extended along the body for a distance of 40 percent of the body length and had a maximum height (increment in radius) of 17 percent of the basic body radius. The bump formed by the addition of the cross-sectional area of the unswept wing extended for a distance of 25 percent of the body length and had a maximum height of 41 percent of the body radius. The bump for the swept wing thus represents a relatively small disturbance on the body, whereas the bump for the unswept wing represents a moderately large disturbance.

Data on the flow fields of the models were obtained on 35-millimeter film in the form of schlieren photographs taken as motion pictures of the flow; these data were obtained for a slowly but continuously increasing Mach number over the speed range, followed by a similar decrease in Mach number. The variable-frequency light source described in reference 3 was used and limited each picture to an exposure of about 4 microseconds. The Mach number for any given photograph was identified by a Mach number indicator that extended into the lower part of the field of observation. The bodies, as previously stated, were mounted at an angle of attack of 0° and the wings on the body were oriented with respect to the optical axis of the schlieren system at 90° , 45° , and 0° . For the 0° view, the wing was along the optical axis of the schlieren system and was not observable in the schlieren pictures.

The tests were conducted over a Mach number range from approximately 0.7 to slightly above 1.0 at a constant stagnation pressure of 20 psia. The corresponding Reynolds number based on body length at a Mach number of 1 was 3×10^6 .

RESULTS AND DISCUSSION

Selected photographs from the motion pictures are presented for the body alone and for the wing-body combinations at Mach numbers of 0.95, 0.98, 1.0, and approximately 1.04, since these photographs cover the Mach number range of shock development. Photographs of the flow past the body alone (fig. 2) show that the body shock begins to form at a Mach number of approximately 0.98 and moves rearward along the body with increasing Mach number. The addition of carborundum on the nose of the body to fix transition of the boundary layer had no effect on the shock pattern nor on the location of the shocks except to produce characteristic disturbance patterns at the roughness location. (Compare figs. 2 and 3.) The similarity of shock formation indicates that the turbulent boundary layer produced by carborundum does not affect the shock formation and that a smooth model may be used throughout the tests without any appreciable effect of sudden transition in the boundary layer on the smooth-nose models.

In order to examine carefully the flow about the wing-body combinations, three views of the flow were made - one taken normal to the span of the wing (90° view), the second taken along the span of the wing (0° view), and the third taken midway between these two (45° view). From an examination of the flow in the three views, the axially symmetrical or dissymmetrical nature of the flow past the wing-body combinations can be determined. The three views of the flow past the 45° swept-wing-body combination and the views of the flow past its equivalent body at Mach numbers from 0.95 to about 1.04 are shown in figure 4. At a Mach number of 0.95 (fig. 4(a)) only minor shocks are observed in the three views and there is close correspondence of the flow past the wing-body and the equivalent body. An increase in the Mach number to 0.98 (fig. 4(b)) produces somewhat stronger shocks; and, again, similar flow conditions are observed on the wing-body combination and equivalent body. At this Mach number the body shock is formed ahead of the wing. At a Mach number of 1.0 (fig. 4(c)), the shock has moved downstream and is located near the wing-tip trailing edge and extends completely across the body. The three views of the flow past the wing-body combination indicate an approximately axially symmetrical type of flow, which is well-reproduced by the equivalent body not only in appearance of shock strength but also in the locations of the body shock ahead of the wing and the main shock. At a Mach number of 1.04, there is some variation in the shock appearance around the body in the wing-body combination or some axial dissymmetry of the shock. This variation is slight, however, and the shock pattern is well-duplicated on the equivalent body. The flow conditions observed past the wing-body combination and its equivalent body indicate that throughout the speed range of the tests the appearance and growth of the shocks on the wing-body combination are well-duplicated on the equivalent body, whose distortion from the basic

body represents a small disturbance. This result indicates equivalence of drag on an untapered sweptback wing-body combination and its equivalent body. The investigation of reference 1 on tapered sweptback wing-body combinations and their equivalent bodies showed good agreement, although the data also indicated that body shape could have some second-order effects.

The flow past the unswept-wing-body combination and its equivalent body is shown in figure 5. At a Mach number of 0.95 (fig. 5(a)), the flow past the wing-body combination appears similar in the different views; thus, approximately axial symmetry of shock formation is indicated. The shock location somewhat ahead of the wing trailing edge is well duplicated on the equivalent body. At a Mach number of 0.98 (fig. 5(b)), the shock is at the trailing edge of the wing and little difference is noted in the three different views of the flow past the body. The shock location is approximately the same as on the equivalent body, yet the equivalent body does produce a small difference in the shock at the shock-body juncture where the shock is forked. At a Mach number of 1.0 (fig. 5(c)), the body shock ahead of the wing occurs near the same location in the three views of the flow past the wing-body combination as on the equivalent body. The main shock behind the wing, however, does show, in the three different views, considerable deviation from axial symmetry. The flow past the equivalent body has the same location of terminal shock and body shock and produces a terminal shock whose shape throughout the field appears to be an average of the variously shaped terminal shocks observed on the wing body. The flow past the equivalent body is an axially symmetrical representation of the axially dissymmetrical flow past the wing-body combination. A similar condition is observed at a Mach number of approximately 1.04 (fig. 5(d)).

These results indicate that, when the wing-body combination gives rise to rapid changes in area along the axis of its equivalent body and represents a moderately large disturbance, axial dissymmetry of the shock formation can occur, yet the equivalent body provides a flow condition that closely corresponds to an integrated effect of the dissymmetry in the aforementioned shock formation. The flow past the equivalent body would be expected to provide increments in drag due to shock that would closely correspond to the increments in drag due to shock on the wing-body combination.

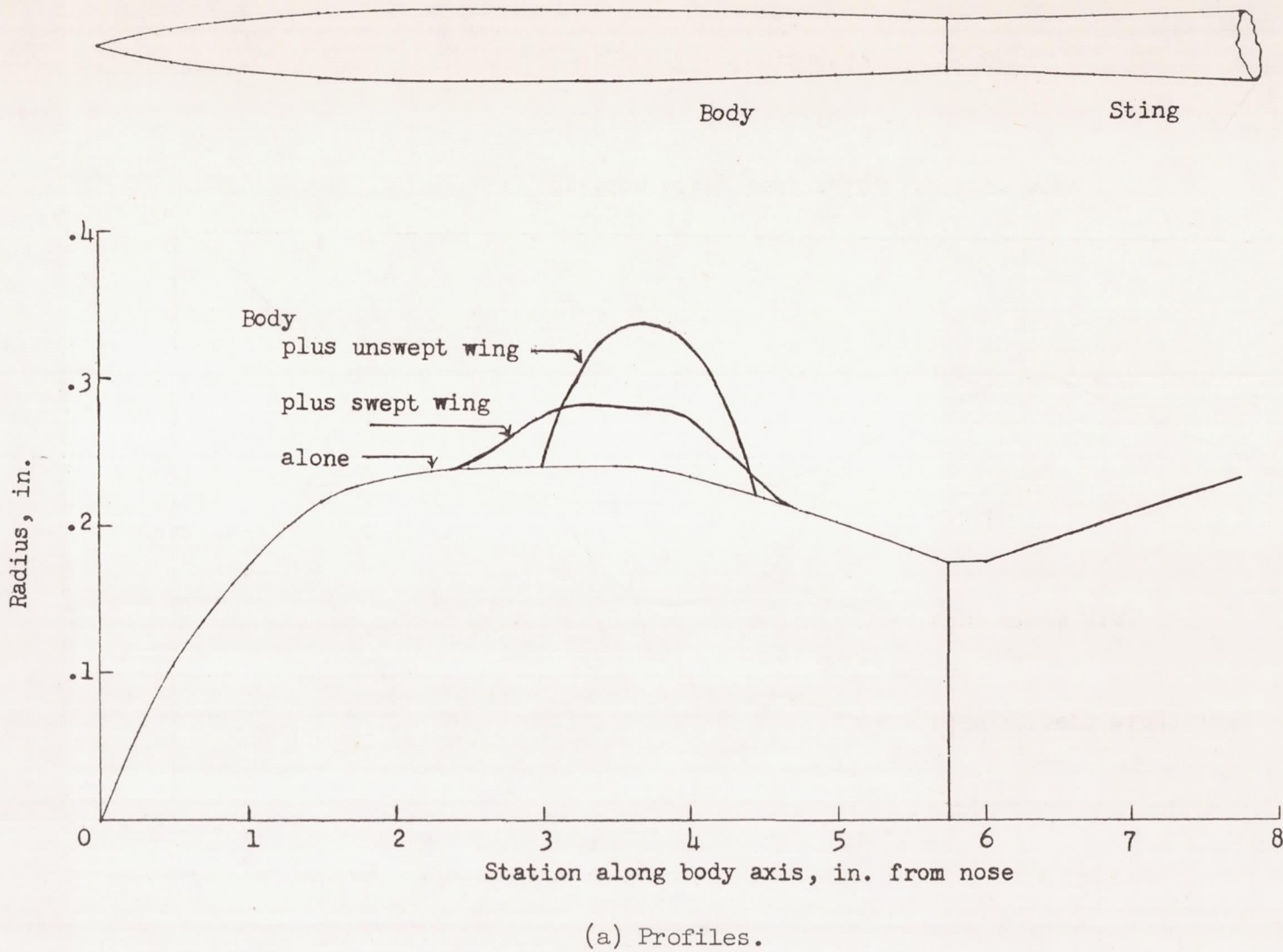
The results of the tests on the two wing-body combinations have indicated that the flow past the equivalent body duplicates or closely approximates that past the wing-body combinations; furthermore, the results indicate that, as the bump representing the wing area on the equivalent body departs radically from a slender bump or small disturbance, the similarity of flow between the wing-body combination and its equivalent body diverges. Presumably, therefore, a wing-body

combination having an unswept wing of aspect ratio greater than 1.5 and thickness-chord ratio greater than 6 percent would not only have considerable axial dissymmetry of the flow past the model, but the differences between the flow past the model and the flow on its equivalent body would be larger than those shown herein.

Langley Aeronautical Laboratory,
National Advisory Committee for Aeronautics,
Langley Field, Va., January 13, 1954.

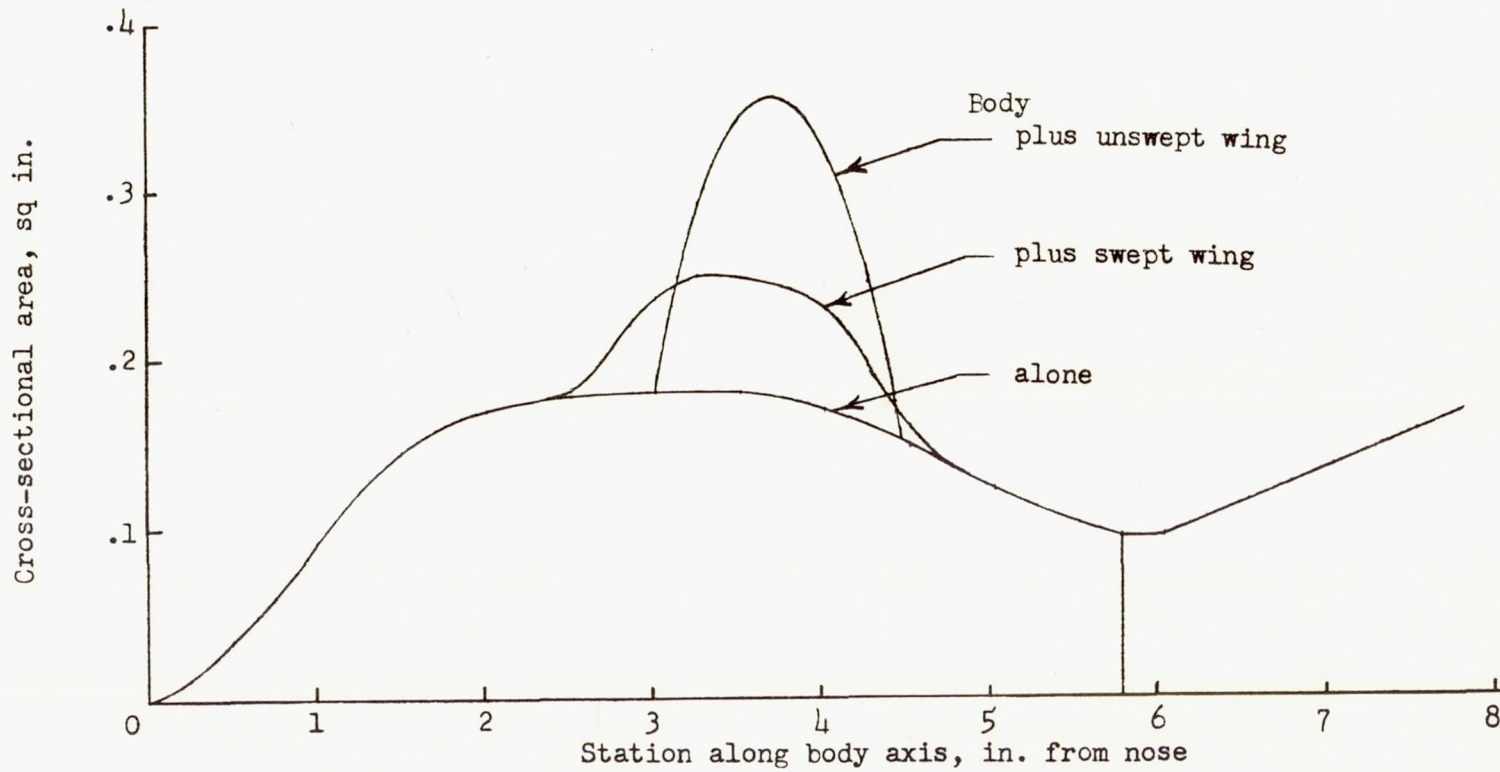
REFERENCES

1. Whitcomb, Richard T.: A Study of the Zero-Lift Drag-Rise Characteristics of Wing-Body Combinations Near the Speed of Sound. NACA RM L52H08, 1952.
2. Daley, Bernard N., and Dick, Richard S.: Effect of Thickness, Camber, and Thickness Distribution on Airfoil Characteristics at Mach Numbers Up to 1.0. NACA TN 3607, 1956. (Supersedes NACA RM L52G31a.)
3. Lindsey, Walter F., and Burlock, Joseph: A Variable-Frequency Light Synchronized With a High-Speed Motion-Picture Camera To Provide Very Short Exposure Times. NACA TN 2949, 1953.



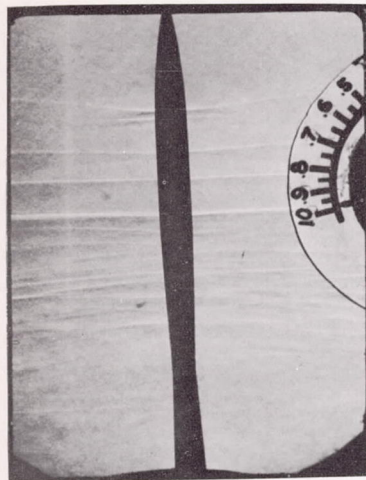
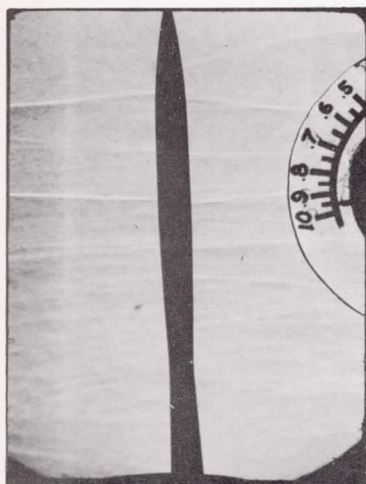
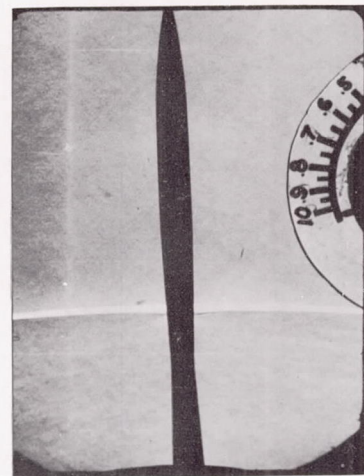
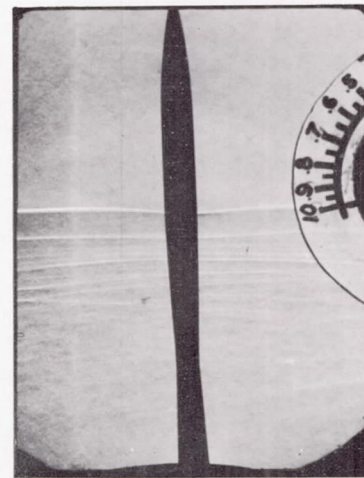
(a) Profiles.

Figure 1.- Profiles and area distributions for body and equivalent bodies.



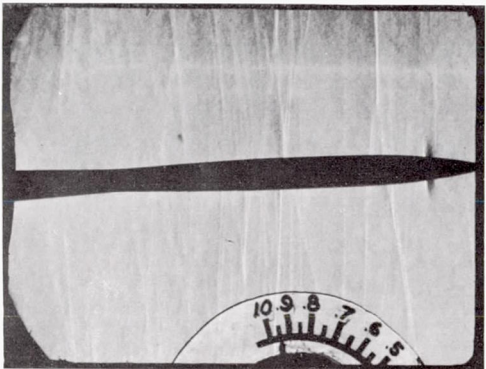
(b) Area distribution.

Figure 1.- Concluded.

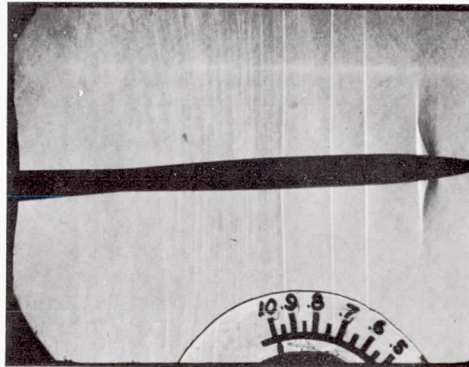
 $M = 0.98$  $M = 0.95$  $M \approx 1.01$  $M = 1.0$

L-82081

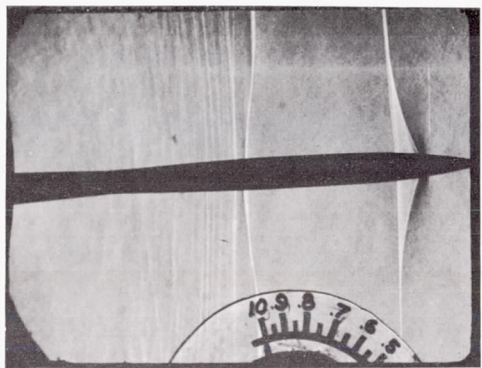
Figure 2.- Body alone.



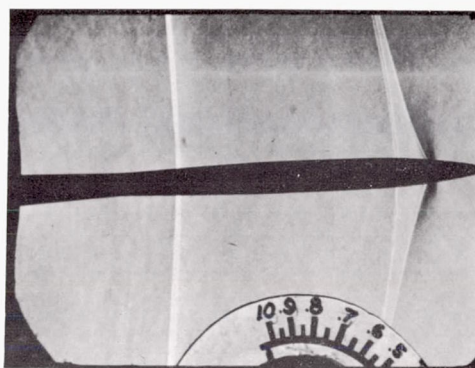
M = 0.95



M = 0.98



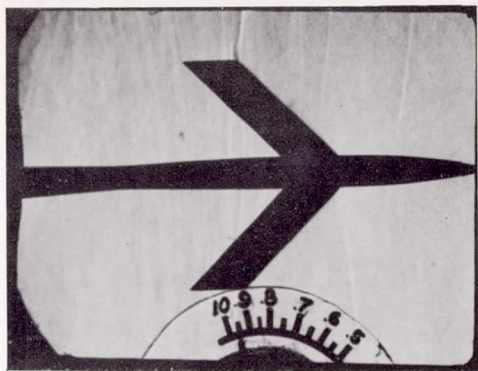
M = 1.0



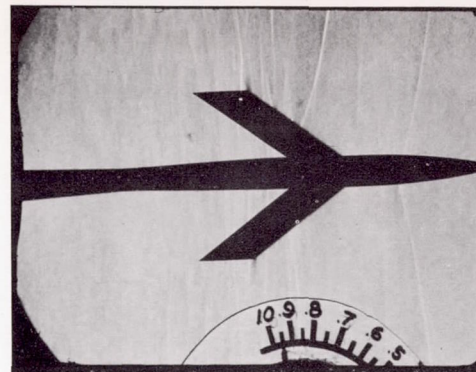
M ≈ 1.04

L-82082

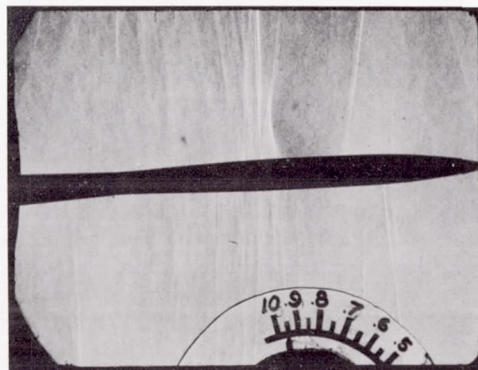
Figure 3.- Body alone with transition strip near nose.



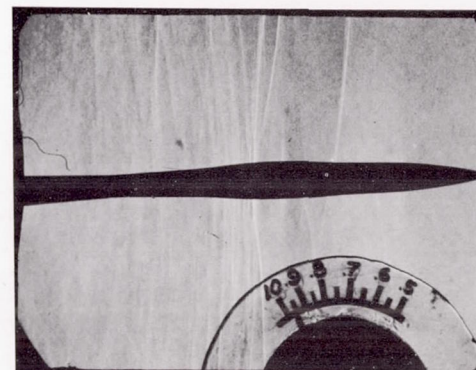
90° view



45° view



0° view

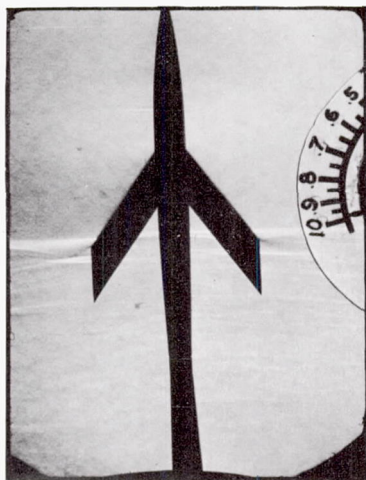


Equivalent body

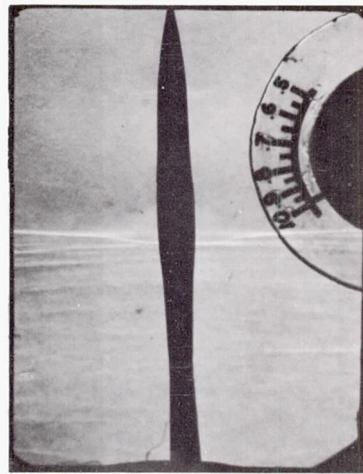
(a) $M = 0.95$.

L-82083

Figure 4.- Body with 45° swept wing.

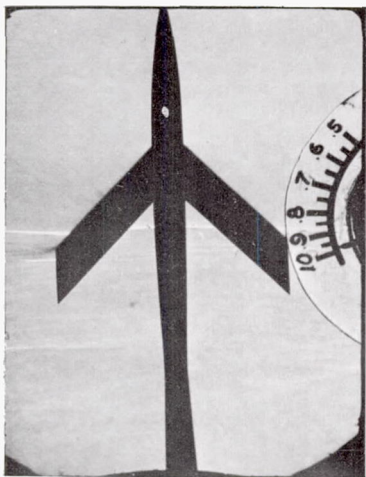


45° view

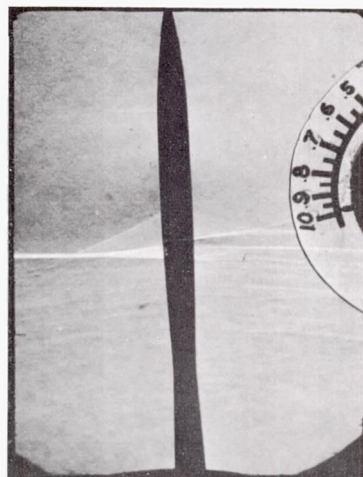


Equivalent body

L-82084



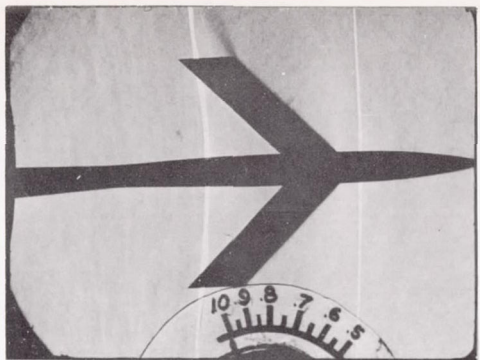
90° view



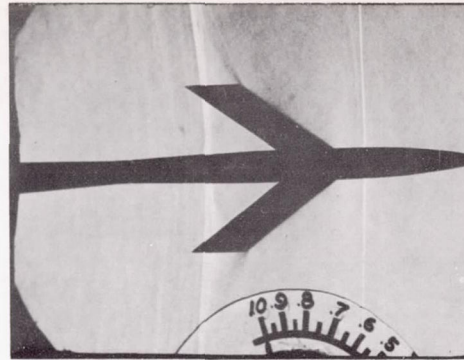
0° view

(b) M = 0.98.

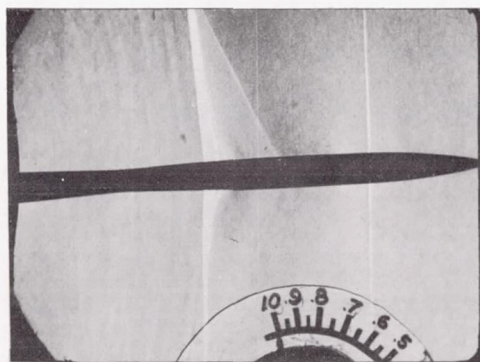
Figure 4.- Continued.



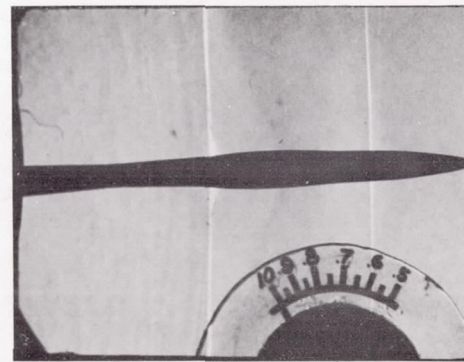
90° view



45° view



0° view

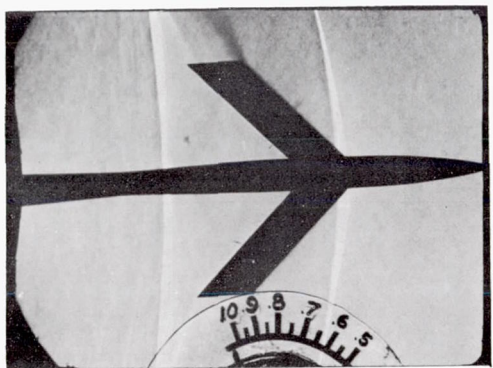


Equivalent body

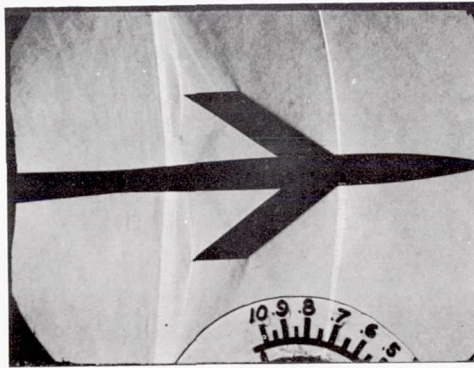
(c) $M = 1.0.$

L-82085

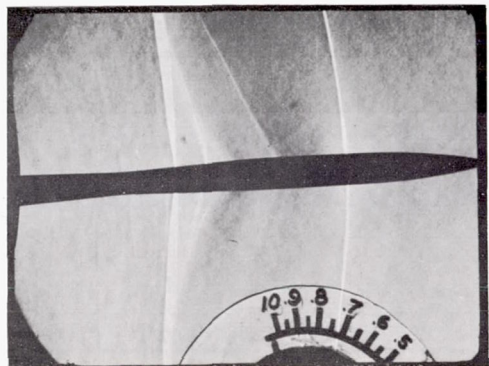
Figure 4.- Continued.



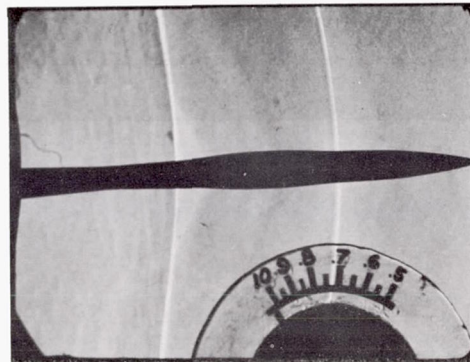
90° view



45° view



0° view

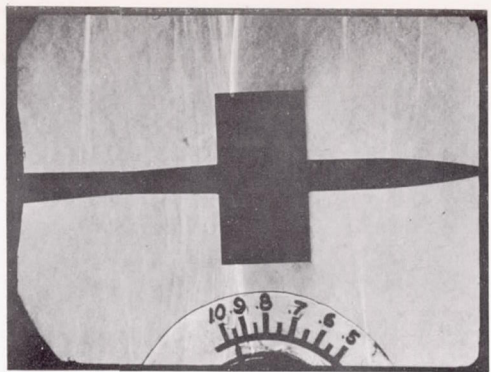


Equivalent body

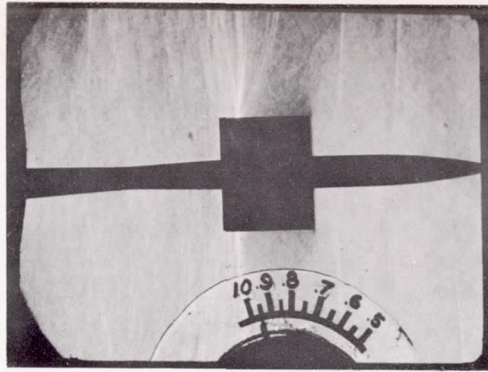
(d) $M \approx 1.04$.

L-82086

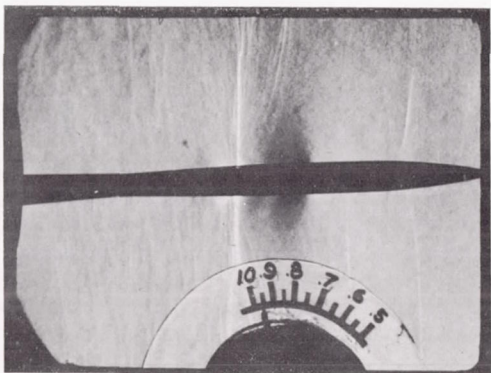
Figure 4.- Concluded.



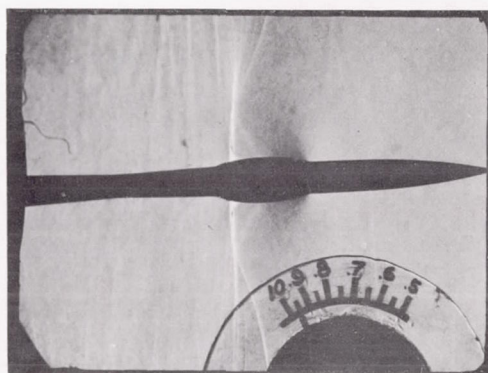
90° view



45° view



0° view

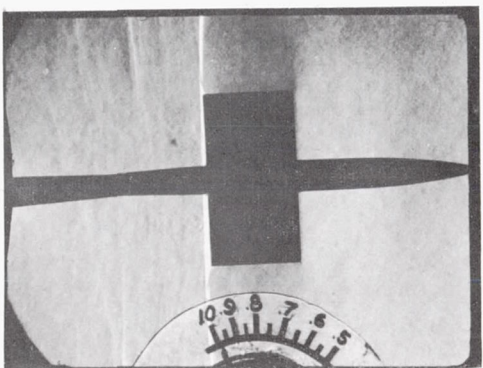


Equivalent body

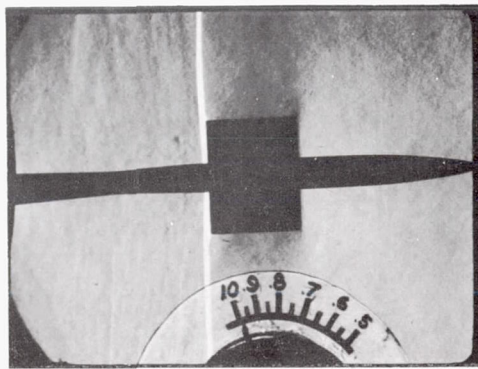
L-82087

(a) $M = 0.95$.

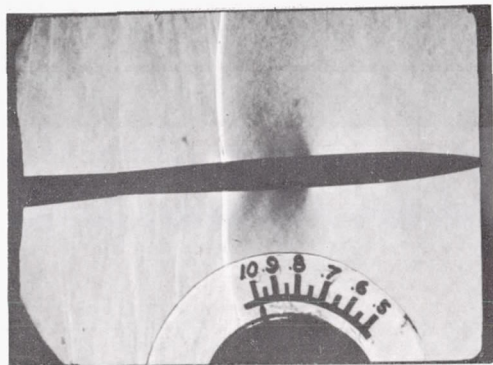
Figure 5.- Body with unswept wing.



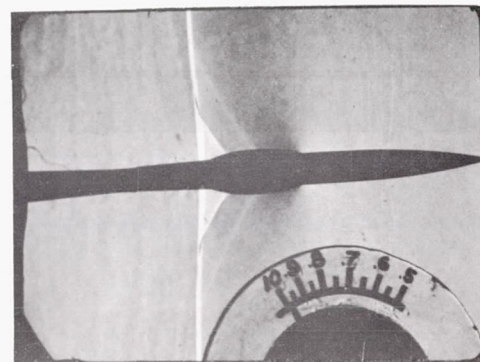
90° view



45° view



0° view

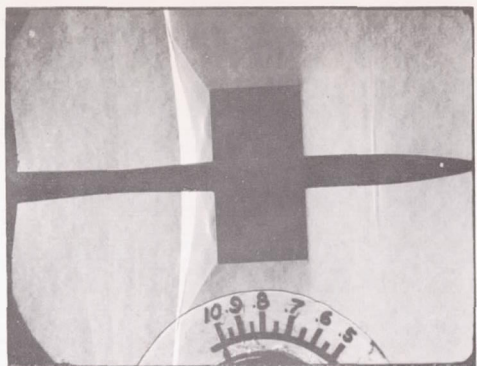


Equivalent body

L-82088

(b) M = 0.98.

Figure 5.- Continued.



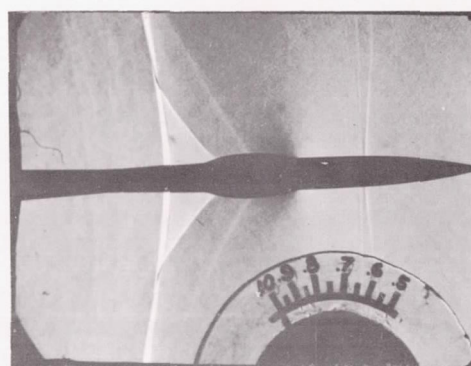
90° view



45° view



0° view

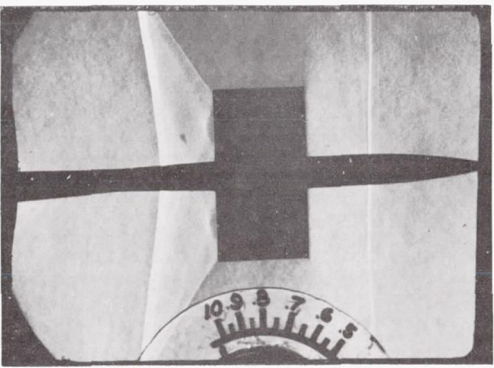


Equivalent body

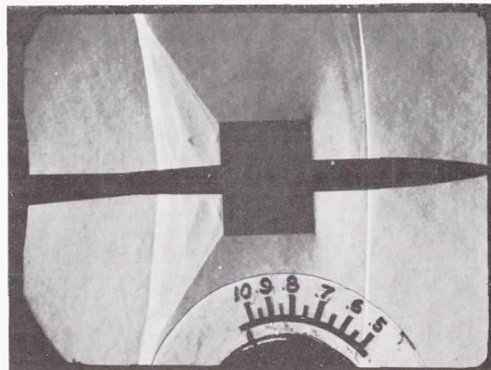
(c) M = 1.0.

L-82089

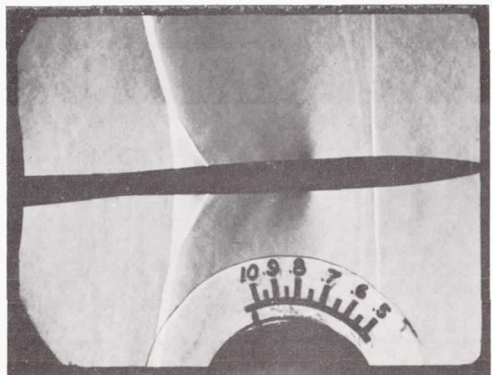
Figure 5.- Continued.



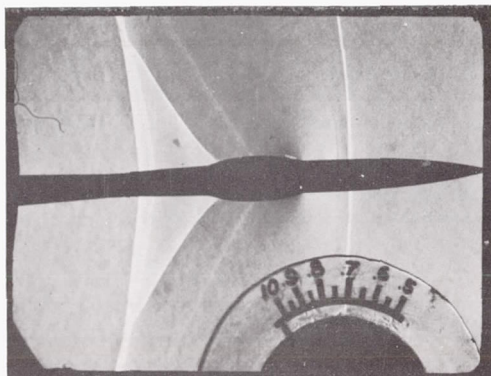
90° view



45° view



0° view



Equivalent body

(d) $M \approx 1.04$.

I-82090

Figure 5.- Concluded.